Date 2011
Author J.H. den Besten and R.H.M. Huijsmans

Address Delft University of Technology
Ship Hydromechanics Laboratory
Mekelweg 2, 2628 CD Delft

TUDelft

Delft University of Technology

Fatigue master curve approach for Arc-Welded aluminium joints – Mean stress effects

by

J.H. den Besten and R.H.M. Huijsmans

Report No. 1797-P 2011

Published in: Proceedings of the ASME 2011 30th International Conference on Ocean, Offshore and Arctic Engineering, OMAE2011, 19- 24 June 2011, Rotterdam, The Netherlands

OMAE 2011 Rotterdam, NL

30th International Conference on Ocean, Offshore and Arctic Engineering
Rotterdam, The Netherlands June 19 - 24, 2011

Technical Symposia

- **Offshore Technology**
- **Structures, Safety and Reliability**
- **Materials Technology**
- **Pipeline and Riser Technology**
- **Ocean Space Utilization**
- **Ocean Engineering**
- **Polar and Arctic Sciences and Technology**
- **CFD and VIV**
- **Ocean Renewable Energy**
- **Offshore Geotechnics**
- **Jan Vugts Symposium on 'Design Methodology of Offshore Structures'**
- **Jo Pinkster Symposium on 'Second Order Wave Drift Forces on Floating Structures'**
- **Johan Wichers Symposium on 'Mooring of Floating Structures in Waves'**

Welcome to the OMAE2011 DVD.

This DVD contains the final papers of the ASME 2011 30th International Conference on Ocean, Offshore and Arctic Engineering. To locate papers, you can do one of the following:

1. Search. You can perform a fielded search of the title, author(s) name, affiliation or paper number.
2. Review the papers listed in the symposia.
3. Browse the Author Index.

This DVD is best viewed with a Java 1.4.2 (or higher) enabled web browser.

You will need Acrobat Reader 7.0 or higher to view the PDF files.

ASME NO-SHOW POLICY

According to ASME's no-show policy, if a paper is not presented at the Conference, the paper will not be

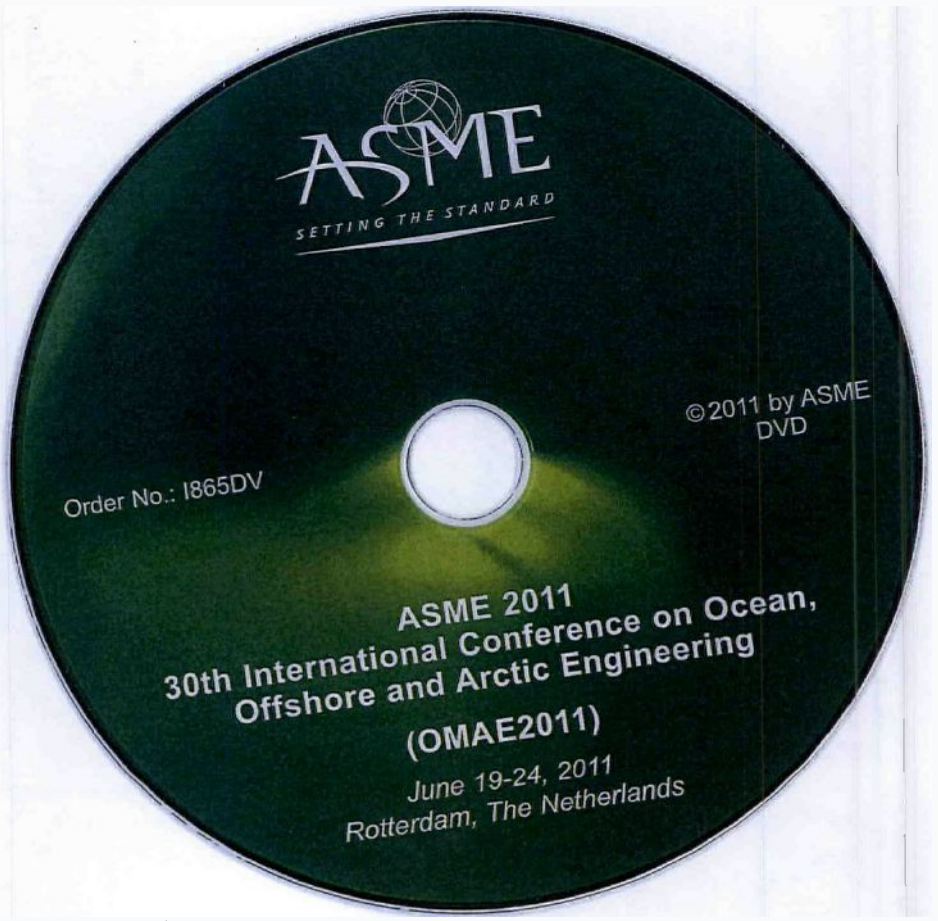
ASME
SETTING THE STANDARD
Order No.: I865DV
©2011 by ASME
DVD
ASME 2011
30th International Conference on Ocean,
Offshore and Arctic Engineering
(OMAE2011)
June 19-24, 2011
Rotterdam, The Netherlands

Proceedings of the ASME 2011 30th International Conference on Ocean, Offshore and Arctic Engineering
OMAE2011
June 19-24, 2011, Rotterdam, The Netherlands

OMAE2011-49733

FATIGUE MASTER CURVE APPROACH FOR ARC-WELDED ALUMINIUM JOINTS ~ MEAN STRESS EFFECTS

J.H. den Besten*
Department of Ship Hydromechanics & Structures
Delft University of Technology
Mekelweg 2, 2628 CD, Delft, The Netherlands
Henk.denBesten@tudelft.nl

R.H.M. Huijsmans
Department of Ship Hydromechanics & Structures
Delft University of Technology
Mekelweg 2, 2628 CD, Delft, The Netherlands
R.H.M.Huijsmans@tudelft.nl

ABSTRACT

Mean stress affects the crack propagation and fatigue performance of arc-welded joints. However, it is a tough phenomenon because of a complex combination of properties in the alternating material zones: weld material, Heat Affected Zone (HAZ) material and base material. First, modeling steps from weld notch stress distributions to weld stress intensity factors, to a non-similitude two-stage crack propagation model, to a fatigue master curve formulation are summarized. Focusing on base and HAZ material, Walker's mean stress model is adopted as a result of a concise review and superior results shown in literature. However, its model coefficient γ is determined using a rational approach rather than curve fitting and a micro- and macro-crack propagation effect is distinguished. Subsequently, for base material, the crack propagation model is modified to incorporate loading induced mean stress effects. Validation using experimental crack propagation data shows promising results. In the HAZ, except loading induced mean stress, the welding process induced residual stress acts as high-tensile mean stress as well. The latter dominates the former in the micro-crack propagation region. Fatigue performance improvement, e.g. a result of Ultrasonic Impact Treatment (UIT), that reduce the high-tensile mean stress is included correcting the loading induced macro-crack propagation mean stress parameter. Finally, the fatigue master curve formulation is modified accordingly and mean stress effects in the HAZ are satisfactorily validated using weld toe failure fatigue test data, including some UIT results.

INTRODUCTION

Important reasons in choosing aluminium to build off-shore support vessels and platform parts like heli-decks are its weight-saving potential, excellent corrosion resistance and welding characteristics. The latter cannot be neglected since arc-welding is the primary joining method. However, it is well-known that arc-welded joints may exhibit poor fatigue properties. Besides, aluminium alloys generally have higher crack propagation rates and smaller (fracture) toughness compared to steel. Taking the dynamic nature of the loading into account, fatigue is a governing damage mechanism and welded aluminium joints are in terms of fatigue often the most critical parts. The maritime innovation project "VOMAS" has been initiated to develop a (high cycle) fatigue design method for the mentioned type of structures. Part of the scope is the development of a fatigue master curve for arc-welded aluminium joints, inspired by the impressive work of Atzori [1,2], Lazzarin [3] and Dong [4,5,6].

Fatigue is concerned with crack initiation and propagation. Governing parameter in the crack initiation period, a surface phenomenon, is the Stress Concentration Factor (SCF). Micro-crack propagation is included in this period because of the low crack propagation rate. When the crack penetrates into the material, the material bulk property induced macro-crack propagation resistance is taking over control. Governing parameter in this crack propagation period is the Stress Intensity Factor (SIF) K. Both parameters, the SCF and SIF, are geometry and loading determined.

For arc-welded structures operating in the high-cycle fatigue region, it is assumed that crack propagation dominates since it is inevitable that flaws already exist. Consequently, the Linear Elastic Fracture Mechanics (LEFM) principles are adopted.

Crack propagation consists of a micro-crack and macro-crack part and both are considered to be important. The micro-crack part in particular because it may constitute a significant part of the fatigue life as a result of the low crack propagation rate. However, the crack propagation rate shows in a number of cases non-similitude behavior in the micro-crack propagation region and even in the lower part of the macro-crack propagation region for base material as well as weld and Heat Affected Zone (HAZ) material. It means that the crack propagation rate is not fully determined by K. This non-similitude behavior might be modeled correcting the macro-crack propagation governing LEFM parameter, the SIF K, for micro-crack propagation using the SCF related weld notch stress distribution.

Consequently, weld notch stress formulations are determined and used to define the weld SIF's for weld toe failure cases and to develop a non-similitude two-stage crack propagation model [7,8]. This model is elaborated into a fatigue master curve formulation [8]. However, mean stress effects are not included yet.

In this paper, the natural steps from weld notch stress distributions to weld stress intensity factors, to a non-similitude two-stage crack propagation model, to a fatigue master curve formulation, are summarized. Different mean stress models and corresponding properties developed over time are shown to explain the model of choice, its parameters and modifications for implementation in the two-stage crack propagation model and fatigue master curve formulation in different material zones. The proposed mean stress model is validated using crack propagation and fatigue test data, for base material (notched plate failure) and HAZ material (weld toe failure) respectively.

WELD NOTCH STRESS DISTRIBUTIONS

Analytical, parametric weld notch stress formulations σ_w (r/t_b) are developed for basic welded joints which take the involved geometry parameters into account [7,8]. These distributions are assumed to be a linear superposition of an equilibrium equivalent part (the linear far field stress) and a self-equilibrating stress part (consisting of a non-linear notch stress: Williams' asymptotic solution and a linear weld geometry induced bending term), as shown in Fig. 1. These stress distributions are related to a far field structural stress amplitude σ_s – obtained using the membrane and bending stress amplitudes σ_m and σ_b and the signs of the corresponding forces $sgn(F_m)$ and $sgn(M_b)$ – and structural bending stress ratio R_s:

$$\sigma_s = \mathrm{sgn}\left(F_m\right)\cdot\sigma_m - \mathrm{sgn}\left(M_b\right)\cdot\sigma_b \tag{1}$$

$$R_s = \mathrm{sgn}\left(M_b\right)\cdot\frac{\sigma_b}{\sigma_s} \tag{2}$$

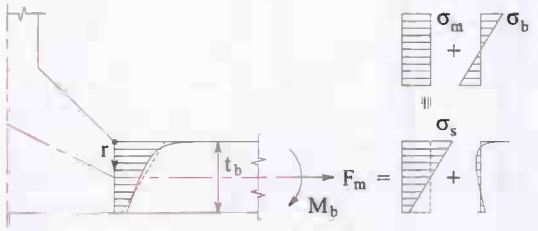

Figure 1. Weld notch stress distribution

WELD STRESS INTENSITY FACTORS

Generalized K solutions for welded joints are not available and hence determined using the equilibrium equivalent stress part related handbook solutions for standard fracture mechanics specimen and a self-equilibrating unit stress part induced correction to cover the weld geometry induced singularity. The mode I SIF, assumed to be dominant, yields:

$$K = \sigma_s \cdot Y_m\left(a\right)\cdot Y_g\left(a\right)\cdot\sqrt{\pi\cdot a} \tag{3}$$

The crack length dependent geometry factor $Y_g(a)$ is related to the equilibrium equivalent stress part and covers the macro-crack part and includes a linear superposition of the membrane and bending contribution. The magnification factor $Y_m(a)$ takes the micro-crack part into account using the (non-linear) self-equilibrating unit stress part.

NON-SIMILITUDE 2-STAGE CRACK PROPAGATION

A cyclic loading introduces a cyclic stress intensity ΔK and may initiate crack propagation. Taking region I as well as region II of a characteristic crack propagation rate curve into account, a Paris equation based non-similitude relation is proposed [7,8]:

$$\frac{da}{dn} = C\cdot Y_m\left(a\right)^{1-\frac{m}{2}}\cdot\left\{\Delta K_g\left(a\right)\right\}^m \tag{4}$$

With:

$$\Delta K_g\left(a\right) = \Delta\sigma_s\cdot Y_g\left(a\right)\cdot\sqrt{\pi\cdot a} \tag{5}$$

For geometries with an initial gap a_g (a crack configuration), like standard crack propagation test specimens and arc-welded joints which typically fail at the weld root (e.g. Partial Penetrated (PP) butt joints and Load Carrying (LC) cruciform joints), Y_m is defined as:

$$Y_m(a) = \frac{Y_n(a)}{Y_l(a)} \tag{6}$$

$Y_n(a)$ is obtained using the non-linear self-equilibrating unit stress; $Y_l(a)$ using the linear unit stress. The SIF K as well as ΔK are for the crack configuration fully determined by Y_g, since the gap (crack) effect is incorporated in the SIF by definition. Y_m is only used to describe the non-similitude crack propagation behavior. In agreement with the uncracked geometry formulation, $Y_l = 0$ for $a_g = 0$ and consequently $Y_m = Y_n$.

FATIGUE MASTER CURVE FORMULATION

Using Eq. (4), separating variables and integration of both sides yields a Basquin type of equation:

$$S_s = C \cdot N^{-\frac{1}{m}} \tag{7}$$

With S_s, a through thickness criterion [8]:

$$S_s = \frac{\Delta\sigma_s}{t_b^{\frac{2-m}{2m}} \cdot I(R_s)^{\frac{1}{m}}} \tag{8}$$

Note that the crack propagation integral $I(R_s)$ is loading and geometry dependent. Dong [6] already introduced the structural stress parameter S_s, however, $I(R_s)$ is not the same as a result of a different σ_s, Eq. (1), magnification factor $Y_m(a)$ and 2-stage crack propagation model, Eq. (4). The fatigue strength coefficient C and slope m have to be determined by experiment.

MEAN STRESS MODELS

At a fixed mean stress level, the number of cycles to failure N decreases for increasing S_s. However, Eq. (7) does not take the (loading induced) mean stress effects explicitly into account. In order to estimate the contribution of mean stress, different models that modify Eq. (7) to a mean stress dependent one are proposed over time.

First, the cyclic stress parameters: the stress range $\Delta\sigma$, the mean value σ_R and the degree of symmetry defined by the mean stress ratio R, have to be determined using the minimum and maximum stress values σ_{min} and σ_{max}:

$$\Delta\sigma = \sigma_{\max} - \sigma_{\min} \tag{9}$$

$$\sigma_R = \frac{\sigma_{\max} + \sigma_{\min}}{2} \tag{10}$$

$$R = \frac{\sigma_{\min}}{\sigma_{\max}} \tag{11}$$

For fatigue induced failure, the maximum (elastic) stress range $\Delta\sigma_{max}$ has to decrease for increasing tensile mean stress σ_R to avoid exceedance of the ultimate strength σ_{us} and the stress amplitude has to satisfy: $\sigma < \sigma_{us}$. Consequently, $C = f(\sigma_R/\sigma_{us})$ is assumed. Fatigue test results suggest a non-linear mean stress dependency and Kwofie [9] proposed an exponential relation:

$$C = f\left(\frac{\sigma_R}{\sigma_{us}}\right) = C_{R-1} \cdot e^{\left\{-\alpha\cdot\left(\frac{\sigma_R}{\sigma_{us}}\right)\right\}} \tag{12}$$

The coefficient C_{R-1} is the fatigue strength parameter corresponding to completely reversed loading: $R = -1$. Using Eq. (7) and Eq. (12) denotes σ for any non-zero mean stress corresponding to the fatigue life N_{R-1}:

$$\sigma = C_{R-1} \cdot e^{\left\{-\alpha\cdot\left(\frac{\sigma_R}{\sigma_{us}}\right)\right\}} \cdot N_{R-1}^{-\frac{1}{m}} \tag{13}$$

The slope m is assumed to be mean stress invariant. For completely reversed loading, the stress amplitude becomes using Eq. 7:

$$\sigma_{R-1} = C_{R-1} \cdot N_{R-1}^{-\frac{1}{m}} \tag{14}$$

The quotient of Eq. (13) and (14) denotes:

$$\frac{\sigma}{\sigma_{R-1}} = e^{\left\{-\alpha\cdot\left(\frac{\sigma_R}{\sigma_{us}}\right)\right\}} \tag{15}$$

A first order approximation of Eq. (15), obtained using a Maclaurin series expansion, yields:

$$\left(\frac{\sigma}{\sigma_{R-1}}\right) = \left\{1 - \alpha\cdot\left(\frac{\sigma_R}{\sigma_{us}}\right)\right\} \tag{16}$$

It has been found that Eq. (16) is a generalization of several empirical mean stress models, developed over time [9,10].

a. For $\alpha = 1$, the linear mean stress dependent Goodman (1899) relation [11] is obtained:

$$\left(\frac{\sigma}{\sigma_{R-1}}\right) = \left\{1 - \left(\frac{\sigma_R}{\sigma_{us}}\right)\right\} \tag{17}$$

Generally speaking, it shows good results for a small mean stress and low (elastic) stress amplitude, typical

in the high-cycle fatigue region: $(\sigma_R/\sigma_{us}) \rightarrow 0$ and $(\sigma/\sigma_{R-1}) \rightarrow 1$.

b. For $\alpha = (\sigma_{us}/\sigma_{ys})$, using the yield stress σ_{ys} instead of the ultimate strength σ_{us} compared to the Goodman relation, the more conservative Soderberg relation [12] appears:

$$\left(\frac{\sigma}{\sigma_{R-1}}\right)=\left\{1-\left(\frac{\sigma_R}{\sigma_{ys}}\right)\right\} \tag{18}$$

c. For $\alpha = (\sigma_R/\sigma_{us})$, the non-linear Gerber (1874) relation [11] shows up:

$$\left(\frac{\sigma}{\sigma_{R-1}}\right)=\left\{1-\left(\frac{\sigma_R}{\sigma_{us}}\right)^2\right\} \tag{19}$$

Generally speaking, it is applied in the low-cycle fatigue region: plastic strain cannot be neglected for increasing (σ_R/σ_{us}) and (σ/σ_{R-1}) and mean stress effects will become non-linear.

Exponential mean stress models have been developed in order to overcome the fatigue induced failure prediction problem in the high-cycle fatigue region with relatively low σ and high σ_R. The Kwofie mean stress model, Eq. (15), can be considered as a generalization of these models.

a. Smith, Watson & Topper [13] proposed the SWT model taking R directly into account. It can be obtained for $\alpha = -\{\sigma_{us}/(2\sigma_R)\} \cdot \ln\{(1-R)/2\}$:

$$\left(\frac{\sigma}{\sigma_{R-1}}\right)=\left(\frac{1-R}{2}\right)^{\frac{1}{2}} \tag{20}$$

b. Walker [14] introduced a comparable model, obtained using $\alpha = -\{\sigma_{us}/(\gamma \cdot \sigma_R)\} \cdot \ln\{(1-R)/2\}$, which contains a fitting parameter γ that substitutes the square root in Eq. (20):

$$\left(\frac{\sigma}{\sigma_{R-1}}\right)=\left(\frac{1-R}{2}\right)^{\gamma} \tag{21}$$

Effective Stress

Using Eq. (7), (12) and (15), an equivalent, effective, completely reversed stress amplitude σ_{eff} can be defined which gives the same fatigue life N as the combination of stress amplitude σ and mean stress σ_R:

$$\sigma_{eff} = C_{R-1} \cdot N^{-\frac{1}{m}} \tag{22}$$

With:

$$\sigma_{eff} = \sigma \cdot e^{\left\{\alpha \cdot \left(\frac{\sigma_R}{\sigma_{us}}\right)\right\}} \tag{23}$$

For the first order approximation, σ_{eff} becomes:

$$\sigma_{eff} = \frac{\sigma}{1-\alpha \cdot \left(\frac{\sigma_R}{\sigma_{us}}\right)} \tag{24}$$

Using Eq. (7) and (23) and the α expression for Walker's model, the effective stress range denotes:

$$\Delta\sigma_{eff} = \frac{\Delta\sigma}{(1-R_s)^{1-\gamma}} \tag{25}$$

Note that $(1/2)^{\gamma}$ as appeared in Eq. (21) is incorporated in the fatigue strength coefficient C.

Walker's model parameter γ, a rational approach

Considering the mentioned mean stress models, Walker's model show superior results [10,15,16] and is decided to be used. It has been found using curve fitting that $\gamma \approx 0.5$ for $R \geq 0$; $\gamma = 0.0$ turned out to be a good assumption for $R < 0$.

Kim and Dong et al. [17] presented a rational approach to take the mean stress into account. It has been assumed that only the tensile part of the stress range $\Delta\sigma^+$ contributes to σ_{eff}, as shown in Fig. 2. The effective stress range is defined as:

$$\Delta\sigma_{eff} = \sqrt{\sigma_{max} \cdot \Delta\sigma^+} \tag{26}$$

Using Eq. 9 and 11, $\Delta\sigma_{eff}$ yields for $R \geq 0$:

$$\Delta\sigma_{eff} = \frac{\Delta\sigma}{(1-R)^{\frac{1}{2}}} \tag{27}$$

Considering $R < 0$, $\Delta\sigma_{eff}$ becomes:

$$\Delta\sigma_{eff} = \frac{\Delta\sigma}{(1-R)} \tag{28}$$

Following this procedure, the effective stress range $\Delta\sigma_{eff}$ is only loading dependent.

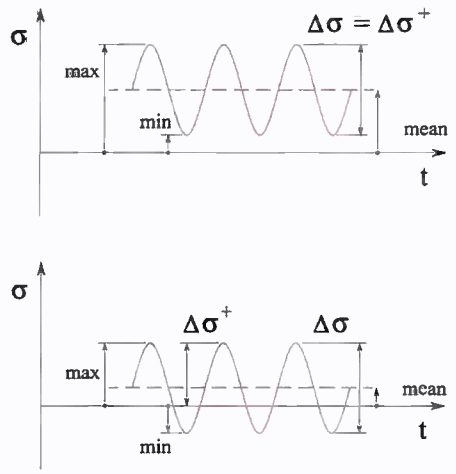

Figure 2. Top: mean stress ratio $R > 0$
Bottom: mean stress ratio $R < 0$

However, comparing Eq. (27) and (28) to (25), it turns out that this rational approach is similar to Walker's model with $\gamma = (1/2)$ for $R \geq 0$ and $\gamma = 0$ for $R < 0$. Hence, these γ values are adopted.

MEAN STRESS EFFECTS

A complex combination of properties in the alternating material zones: weld material, Heat Affected Zone (HAZ) material and base (parent) material, as shown in Fig. 3 for a Single Sided (SS) butt joint, influences the fatigue performance of arc-welded joints.

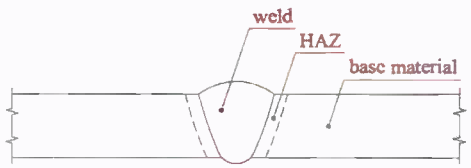

Figure 3. Alternating material zones

For base material, the mean stress is loading induced. However, in the HAZ, the important material zone for weld toe failure, the welding process induced residual stress act as high tensile mean stress (at yield magnitude) as well. To include both, the loading and welding process induced part, a superposition is required. Although, the latter is proposed to be left in the fatigue strength constant C for now and only loading induced mean stress is explicitly taken into account. The weld material zone, important for weld root failure, is left out of consideration to focus on mean stress effects in base material in comparison to HAZ material only.

If at some day a fatigue master curve formulation is required that covers both base material (notched plate failure) as well as HAZ material (weld toe failure), the welding induced residual stress have explicitly to be taken into account as well. A modification of Williams' asymptotic solution as part of the weld notch stress distribution (a micro-crack propagation region correction!) for heat input developed by Lazzarin et al. [18] has to be mentioned.

Now, constant amplitude loading induced mean stress effects are investigated for base material using crack propagation data; for HAZ material using fatigue data of basic welded geometries, failed at the weld toe.

Base Material

It is assumed that the loading induced mean stress affects both the micro- and macro crack propagation region. Modifying the non-similitude two-stage crack propagation model (4) using the effective stress range according to Walker's model (25) yields:

$$\frac{da}{dn} = C \cdot \frac{Y_m}{(1-R_s)^{1-\gamma}} \cdot \left\{ \frac{Y_m^{-\frac{1}{2}}}{(1-R_s)^{\frac{1-\gamma}{2}}} \cdot \Delta K_g \right\}^m \qquad (29)$$

The square root behavior of the mean stress is naturally included according to the micro- and macro-crack propagation related magnification factor Y_m.

The proposed model (29) has been verified using experimental crack propagation data of aluminium 5083 Centre Cracked Tension (CCT) specimens in T-L configuration, published by Sonsino [19].

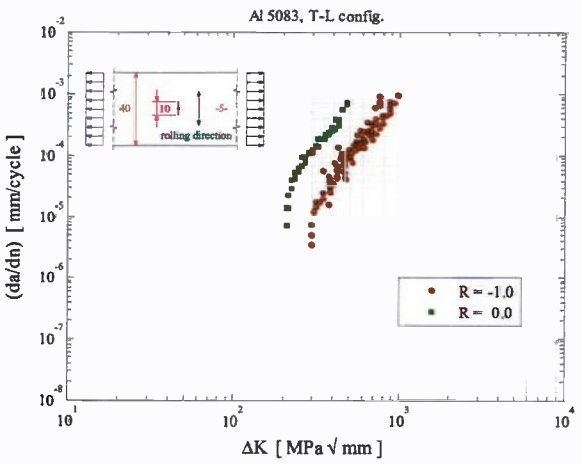

Figure 4. CCT specimen, (da/dn) - ΔK data [13].

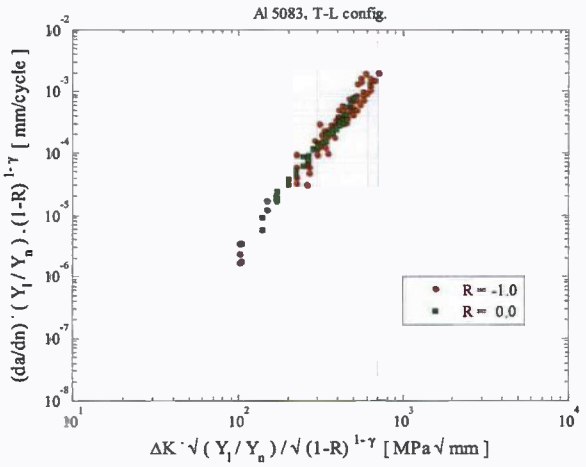

Figure 5. CCT specimen, (da/dn) - ΔK data [13] using crack propagation model (29).

Two data sets were provided at different mean stress ratios: R = -1.0 [-] and R = 0.0 [-]. The original data contains some non-similitude behavior and mean stress effects as shown in Fig. 4. The model results are shown in Fig. 5. Note that the non-similitude part at the right hand side of Eq. (29) is moved to the left to present the data in single slope region II behavior.

High strength aluminium 2024 CCT specimen and 7075-T651 Compact Tension Test (CTT) specimen crack propagation data is used for validation as well, published by Tenpierik [20] and Jiang et al. [21] respectively. The original data is shown Fig. 6 and 8; model results are presented in Fig. 7 and 9.

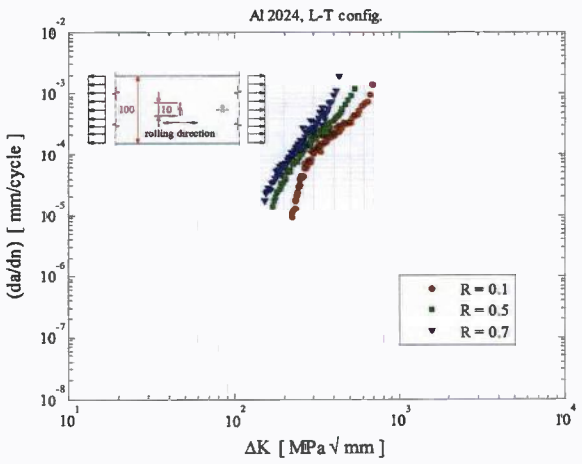

Figure 6. CCT specimen, (da/dn) - ΔK data [14].

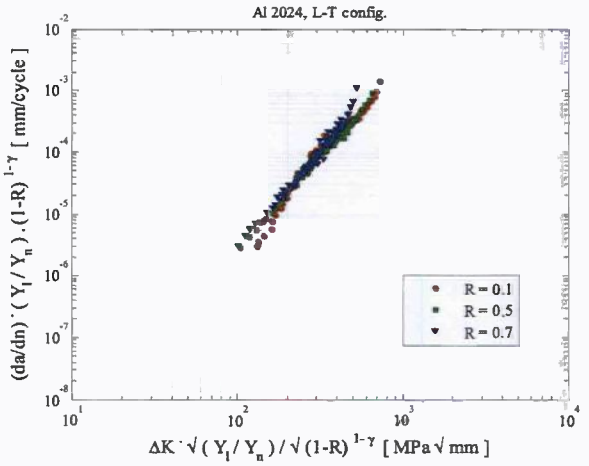

Figure 7. CCT specimen, (da/dn) - ΔK data [14] using crack propagation model (29).

Heat Affected Zone (HAZ) Material

As the HAZ is in between base material and weld material, it is constraint. The welding process induced residual stress is highly tensile in the micro-crack region, dominates the loading induced mean stress no matter its level and decreases in the macro-crack region. Assuming that the residual stress effects are approximately the same for all welded joints, the loading induced mean stress part is ignored in the micro-crack region. Modifying Eq. (29) accordingly and using the Basquin equation (7), the stress parameter S_s becomes:

$$S_R = \frac{\Delta\sigma_s}{(1-R)^{\frac{1-\gamma}{2}} \cdot t_b^{\frac{2-m}{2m}} \cdot I(R_s)^{\frac{1}{m}}} \tag{30}$$

Note that in [17] the mean stress correction is proposed (only) to be included in the micro-crack propagation region.

To reduce the high-tensile mean stress in the micro-crack region and improve the welded joint fatigue performance, peening techniques or Ultrasonic Impact Treatment (UIT) can be used. The effects may be taken into account by introducing a mean stress improvement (technique dependent) ratio R_i in the micro-crack region. For very effective techniques, $R_i \rightarrow -\infty$. However, fatigue induced failure requires that at least a small part of the stress cycle is in tension. Quantifying R_i is not an easy task and hence it is estimated comparing as-welded and improved welded joints. Consequently, R_i is a relative parameter and prevents for the definition of a welding induced high-tensile mean stress ratio. To maintain the S_R formulation (30), an equivalent mean stress ratio R_{eq} is defined:

$$R_{eq} = 1-(1-R)\cdot(1-R_i)^{\frac{2\cdot(1-\gamma_I)}{m\cdot(1-\gamma)}} \tag{31}$$

For verification purposes, some fatigue test data series for basic welded geometries [22,23,24]: T-joints, butt joints and longitudinal stiffener joints are considered to highlight the mean stress effects. The effects of improved fatigue performance using UIT is included as well using the test data published by Haagensen [25]. The 2-parameter curve fitted nominal stress data is shown in Fig. 10. The scatter range index $T_\sigma = 1:\{\sigma(P_s = 10[\%])/\sigma(P_s = 10[\%])\}$ is quite large. One of the major causes in scatter in fatigue data is the welding induced second order bending stress, which is not the same for the different data series. It is decided to take it into account for the master curve formulation if this information is available. Fig. 11 and 12 show respectively the model results excluding and including mean stress effects.

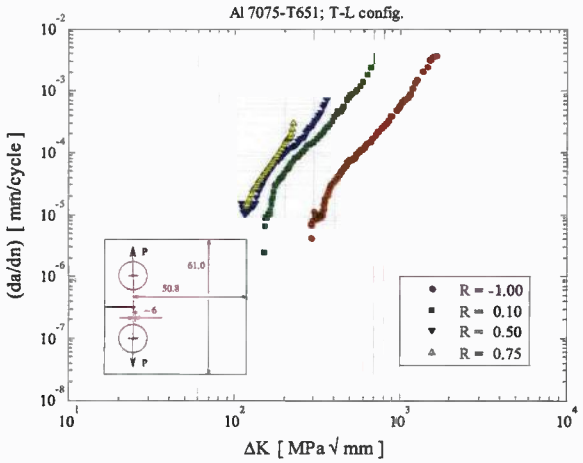

Figure 8. CTT specimen, (da/dn) - ΔK data [15].

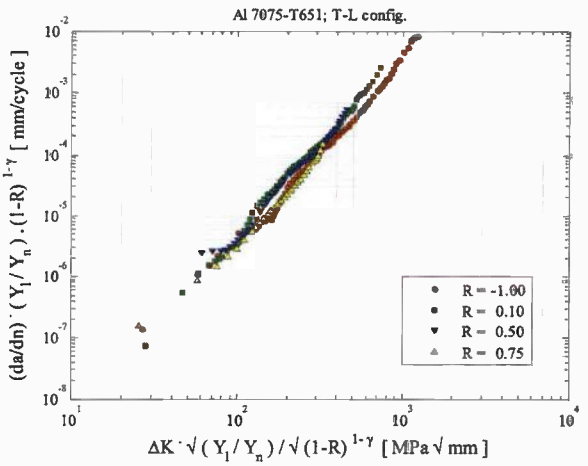

Figure 9. CTT specimen, (da/dn) - ΔK data [15] using crack propagation model (29).

Data analysis demonstrated that $R_i \approx -1.5$ [-] in this particular case, meaning that $\Delta\sigma^+ = (4/10)\cdot\Delta\sigma$. It turns out that the high-tensile mean stress is not only reduced but even altered to a compressive one.

Including more fatigue test data results [26,27,28,29,30] provides Fig. 13. It contains only weld toe failure cases for aluminium 5000 and 6000 series arc-welded joints in basic geometries. The base plate thickness $t_b = 3.0 \ldots 25.0$ [mm]; the loading induced mean stress ratio $R = -1 \ldots 0.5$ [-]. The $(\mu\text{-}2\sigma)$ line is included for convenience; the slope $m = 3.4$ [-].

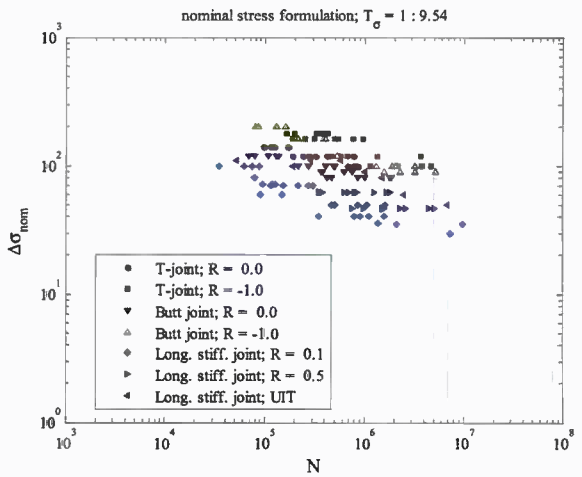

Figure 10. Fatigue nominal stress formulation.

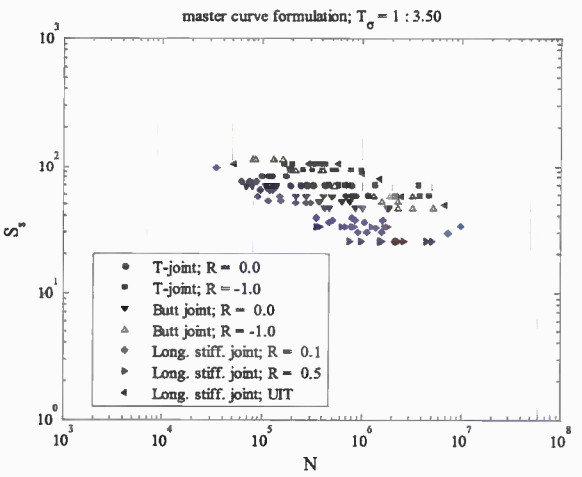

Figure 11. Fatigue master curve formulation, mean stress effects not included.

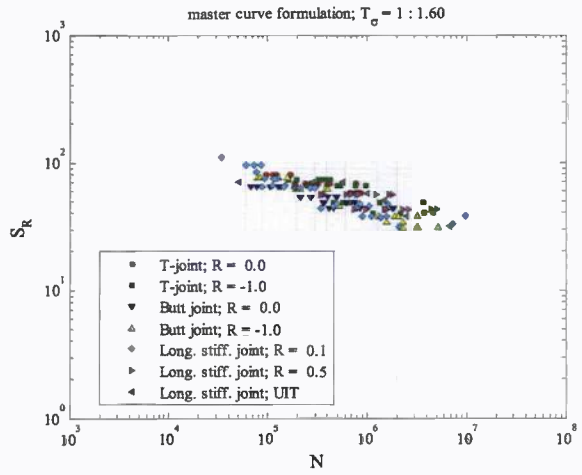

Figure 12. Fatigue master curve formulation, mean stress effects included.

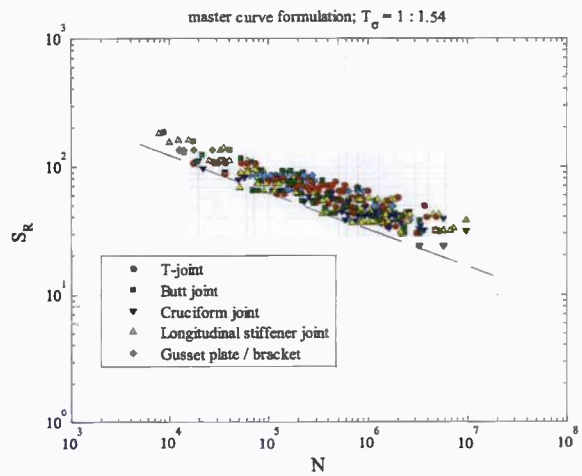

Figure 13. Fatigue master curve formulation; weld toe failure cases for arc-welded joints in basic geometries, mean stress effects included; (μ-2σ) - line is shown for convenience, m = 3.4 [-].

CONCLUSIONS

Mean stress affects the crack propagation and fatigue performance of arc-welded joints. However, it is a tough phenomenon because of a complex combination of properties in the alternating material zones: weld material, HAZ material and base material. The different zones are respectively important for weld root failure, weld toe failure and notched plate failure cases.

Focusing on base material and HAZ material, Walker's mean stress model has been adopted because of the superior results shown in literature. However, its model coefficient γ is determined using a rational approach, rather than curve fitting, assuming that only the tensile part of the stress cycle contributes to fatigue structural damage.

For base material, mean stress is loading induced and it influences the micro- as well as the macro-crack propagation region. The non-similitude two-stage crack propagation model (29) has been modified accordingly. Validation using experimental crack propagation data of aluminium standard specimens, obtained at mean stress ratios R = -1.0 ... 0.7 [-], show promising results.

In the HAZ, important for weld toe failure cases, except loading induced mean stress, the welding process induced residual stress act as high tensile mean stress (at yield magnitude) as well. In the micro-crack propagation region, it dominates the loading induced part no matter its level. Assuming that it is approximately similar for all welded joints, it is not explicitly considered and its effect is proposed to be left in the fatigue strength constant C. Consequently, the loading induced mean stress is ignored in the micro-crack propagation region and only taken into account in the macro-crack propagation region. The fatigue master curve formulation (30) is modified accordingly. However, fatigue performance improvement techniques like UIT that reduce the welding induced high-tensile mean stress in micro-crack propagation region exist. Hence, an equivalent mean stress ratio R_{eq} is introduced to correct for these effects. The improvement technique dependent mean stress ratio R_i, a relative parameter, is based on comparison of as-welded and improved arc-welded joint fatigue test results. HAZ material mean stress effects are satisfactorily validated using weld toe failure fatigue test data of welded joints at different mean stress ratios R = -1.0 ... 0.5 [-], including some UIT fatigue performance improvement results.

ACKNOWLEDGMENTS

The authors would like to thank the project participants: Damen Shipyards, research institutes MARIN and TNO, classification societies Bureau Veritas and Lloyds Register and the US Coast Guard for funding this research. In addition, the authors are grateful to C.M. Sonsino and Y. Jiang for providing the experimental crack propagation data.

REFERENCES

[1] Atzori, B. et al., 1997. "Stress Distributions for V-shaped Notches Under Tensile and Bending Loads". *Fatigue & Fracture of Eng. Materials*, 20, pp. 1083-1092.

[2] Atzori, B. et al., 2005. "Stress Distributions in Notched Structural Components under Pure Bending and Combined Traction and Bending". *Fatigue & Fracture of Eng. Materials*, 28, pp. 13-23.

[3] Lazzarin, P. et al., 1996. "A Unified Approach to the Evaluation of Linear Elastic Stress Fields in the Neighborhood of Cracks and Notches". *Int. J. of Fracture*, 78, pp. 3-19.

[4] Dong, P., 2001. "A Structural Stress Definition and Numerical Implementation for Fatigue Analysis of Welded Joints". *Int. J. of Fatigue*, 23, pp. 865-876.

[5] Dong, P., 2003. "A Robust Structural Stress Method for Fatigue Analysis of Ship Structures". *Proc. 22nd Int. Conf. on Offshore Mechanics and Arctic Engineering*, OMAE 2003, Cancun, Mexico.

[6] Dong, P. et al., 2003. "Stresses and Stress Intensities at Notches: 'Anomalous Crack Growth' Revisited". *Int. J. of Fatigue*, 25, pp. 811-825.

[7] Besten, J.H. den, Huijsmans, R.H.M., 2010. "Fatigue in High-Speed Ships: Crack Propagation in Aluminum". *Proc. 11th Int. Symp. on Practical Design of Ships and Other Floating Structures*, PRADS 2010, Rio de Janeiro, RJ, Brazil.

[8] Besten, J.H. den, Huijsmans, R.H.M., 2011. "Fatigue in High-Speed Ships: a Master Curve Formulation". *Proc. 3rd Int. Conf. on Marine Structures*, MARSTRUCT 2011, Hamburg, Germany.

[9] Kwofie, S., 2001. "An Exponential Stress Function for Predicting Fatigue Strength and Life due to Mean Stresses". *Int. J. of Fatigue*, 23, pp. 829-836.

[10] Lobato da Silva, B. et al., 2010. "Influence of Mean Stress on the Fatigue Strength of ASTM A743 CA6NM Alloy Steel". *Frattura ed Integrità Strutturale*, 14, pp. 17-26.

[11] Dowling, N.E., 2007. *Mechanical Behavior of Materials*, 3rd edition, Prentice Hall, Englewood Cliffs.

[12] Herzberg, R.W., 1995. *Deformation and Fracture Mechanics of Engineering Materials*, 44th ed., Wiley, John & Sons.

[13] Smith, K.N., Watson, P., Topper, T.H., 1970. "A stress-strain function for the fatigue of metals". *J. of Materials*, 4, pp. 767-778.

[14] Walker, K., 1970. "The Effects of Stress Ratio During Crack Propagation and Fatigue for 2024-T3 and 7-075-T6 Aluminum". Effects of Environment and Complex Load History on Fatigue Life, ASTM STP 462, pp. 1-14.

[15] Mann, T., 2007. "The Influence of Mean Stress on Fatigue Crack Propagation in Aluminium Alloys". *Int. J. of Fatigue*, 29, pp. 1393-1401.

[16] Dowling, N.E. et al., 2009. "Mean Stress Effects in Stress-Life Fatigue and the Walker Equation". *Fatigue & Fract. of Engineering Materials & Structures*, 32, pp. 163-179.

[17] Kim, J.S., Dong, P. et al., 2006. "Mean Load Effect on Fatigue Welded Joints Using Structural Stress and Fracture Mechanics Approach". *Nuclear Engineering and Technology*, 38, pp. 277-284.

[18] Lazzarin, P. et al., 2005. "Generalized Stress Intensity Factors due to Steady and Transient Thermal Loads with Applications to Welded Joints". *Fatigue & Fract. of Engineering Materials & Structures*, 29, pp. 440-453.

[19] Sonsino, C.M., et al., 1999. "Fatigue Assessment of Welded Joints in AlMg 4.5Mn Aluminium Alloy (AA5083) by Local Approaches". *Int. J. of Fatigue*, 21, pp. 985-999.

[20] Zuidema, J., Veer, F.A., Tenpierik, M.J., Kranenburg, C. van, 2001. "Onderzoek naar verschillende invloeden op de scheurgroeisnelheid bij vermoeiing van aluminium AA 2024", report, Delft University of Technology, Delft.

[21] Jiang, Y., et al., 2008. "A Study of Fatigue Crack Growth of 7075-T651 Aluminum Alloy". *Int. J. of Fatigue*, 30, pp. 1169-1180.

[22] Morgenstern, C., 2006. "Kerbgrundkonzepte für die schwingfeste Auslegung von Aluminium schweiß-verbindungen am Beispiel der naturhärteten Legierung AlMg4,5Mn (AW-5083) und der warmausgehärteten Legierung AlMgSi1 T6 (AW-6082 T6)". Fraunhofer-Institut für Betriebsfestigkeit (LBF), Darmstadt. LBF-report No. FB-231.

[23] Matic, T., Domazet, Z., 2005. "Determination of Structural Stress for Fatigue Analysis of Welded Aluminium Components Subjected to Bending". *Fatigue & Fract. of Engineering Materials & Structures*, 28, pp. 835-844.

[24] Straalen, IJ.J., Soetens, F., Dijkstra, O.D., 1994. "EUREKA 269 – Fatigue Test on Longitudinal Non-Load Carrying Fillet Welds". TNO-report 94-CON-R1566. TNO Building and Construction Research.

[25] Haagensen, P. J., et al., 1998. "Introductory fatigue tests on welded joints in high strength steel and aluminium improved by various methods including ultrasonic impact treatment (UIT)". IIW Doc. XIII-1748-98.

[26] Straalen, IJ.J., Soetens, F., Dijkstra, O.D., 1994. "EUREKA 269 – Fatigue Test on Transverse Butt Welds". TNO-report 94-CON-R1563. TNO Building and Construction Research.

[27] Straalen, IJ.J., Soetens, F., Dijkstra, O.D., 1994. "EUREKA 269 – Fatigue Test on Transverse Non-Load Carrying Fillet Welds". TNO-report 94-CON-R1565. TNO Building and Construction Research.

[28] Maddox, S.J., 1995. "Scale Effect in Fatigue of Filled Welded Aluminium Alloys". *Proc. 6th Int. Conf. on Aluminium Weldments*, Miami,FL, USA.

[29] Meneghetti, G., et al., 1997. "Experimental Analysis of the Fatigue Strength of Welded Structural Details in Aluminium Alloy". *Proc. of the 26th AIAS Nat. Conf.*, Catania, Italy.

[30] Tveiten, B.W., 1999. "Fatigue Assessment of Welded Aluminum Ship Details". PhD thesis, Norwegian University of Science and Technology, Trondheim.